

# Irradiation and flame retardant effect of poly[bis(phenoxyphosphazene)] and magnesium hydroxide in LDPE composites<sup>\*</sup>

LI Jian-Xi (李建喜),<sup>1,2</sup> Zhang Cong (张聪),<sup>1</sup> CHEN Tao (陈涛),<sup>1</sup> LI Lin-Fan (李林繁),<sup>1</sup> and LI Jing-Ye (李景烨)<sup>1,†</sup>

<sup>1</sup>CAS Center for Excellence on TMSR Energy System, Shanghai Institute of Applied Physics,  
Chinese Academy of Sciences, Shanghai 201800, China

<sup>2</sup>University of Chinese Academy of Sciences, Beijing 100049, China

(Received January 19, 2015; accepted in revised form March 16, 2015; published online June 20, 2015)

Poly[bis(phenoxyphosphazene)] (PBPP) and magnesium hydroxide (MH) are used as a flame retardant blend with low-density polyethylene (LDPE) for the nuclear cable. This study aims to investigate the effects of PBPP in MH-LDPE blend composites on flame retardance and electron beam irradiation. The structure, morphology, and properties of the blend composites irradiated by an electron beam to different absorbed doses were characterized. The results indicated that PBPP provides lubrication during processing. As the PBPP content in the blend increases the melt flow rate at 20 phr MH, meaning the material is easier to process. The higher the PBPP content, the higher the limiting-oxygen index. The elongation at the break of the PBPP containing composites (at 50 phr MH) was evidently higher than the non-PBPP ones at different absorbed doses by electron beam irradiation. The thermogravimetric analysis results indicated that the improved mechanical property, resulting from electron-beam irradiation, could be attributed to the consumption of PBPP.

Keywords: Flame retardant, Electron beam irradiation, Low-density polyethylene, Poly[bis(phenoxyphosphazene)], Magnesium hydroxide

DOI: 10.13538/j.1001-8042/nst.26.030304

## I. INTRODUCTION

Low density polyethylene (LDPE) plays an important role in plastics industry due to its excellent properties, such as good mechanical properties, good resistance to chemicals, and easiness to process [1, 2]. However, it is flammable. People have done a lot of research to improve the flame retardancy of LDPE. There are two approaches to achieve flame retardancy in polymers, generally known as the ‘additive’ type and the ‘reactive’ type [3]. Additive type flame retardants are widely used in LDPE, mainly as follows: (1) Inorganics: nano-clay, metal oxide, and metal hydroxide were employed to fill the polymer matrix. However, high loading results in lower mechanical properties of the flame-retardant materials due to poor compatibility. (2) Organics: most of the organic additives are halogen-containing flame retardants [4]. However, they are toxic to the environment and humans during combustion. Thus, alternatives to halogen-containing flame retardants are in demand.

Generally, it is believed that the combustion of a polymer is affected by five factors — primary elements, heat, oxygen, combustible materials, and radical reactions. Polymer combustion in air can be divided into three stages: (1) the thermal decomposition of the polymer produced flammable gas, (2) the flammable products combust in the air, (3) part of the heat produced by combustion promotes the continued breakdown and burning of solid or molten materials. The role of flame retardants is to abort one or two of the three stages, which achieves the purpose of preventing or slowing combustion.

The range of phosphorus containing flame retardants is extremely wide and the materials are versatile. Reactions of phosphorus containing flame retardants occur in combustion as follows, phosphorus compounds – phosphoric acid – metaphosphoric acid – metaphosphoric acid copolymer [5]. Where, the generated metaphosphoric acid copolymer is a vitreous substance which forms a protective film covering the cumbering zone to cut off oxygen. The generated phosphoric acid and metaphosphoric acid copolymer have strong dehydration and carbonization properties. The carbonized layer can block oxygen diffusion to prevent combustion. Meanwhile, the poor thermal conductivity of the carbonized layer, which can prevent heat transfer between the internal polymer and the external heat source, plays an important role in slowing thermal decomposition. In addition, phosphorus containing flame retardants generating PO· radicals through heat can substantially absorb H· and HO· radicals, thereby interrupting the combustion reaction. The flammability of nitrogen containing flame retardants is not good, as a result, usually they are used with phosphorus flame retardants. The nitrogen containing compounds can promote carbonization of phosphorus containing compounds. Thus, nitrogen-phosphorus flame retardants exhibit a synergistic effect [6].

Poly(phosphazene)s are inorganic-organic hybrid polymers, in which the inorganic element is incorporated with the organic backbone, or side chain. Poly[bis(phenoxyphosphazene)] (PBPP) is a good candidate for a flame retardant [7–10]. The alternation of the double bonds,  $-N=P-N=P-$ , in the backbone constitute a system with a  $\pi-\pi$  conjugated structure. Such conjugated structures can resist electron beam irradiation and protect the polymer matrix [11–15]. Meanwhile, there are two groups in every repeating unit and a P–N typed synergistic effect.

\* Supported by the “Strategic Priority Research Program” of the Chinese Academy of Sciences (No. XDA02040300)

† Corresponding author, jingyeli@sinap.ac.cn

These polymer composites can be introduced into materials used in nuclear fields because of their excellent flame retardant properties, but there is still a lack of special study on nuclear power station cable applications in China [16, 17]. In this work, the PBPP-MH-LDPE (MH: magnesium hydroxide) composites were studied for flame retardant and resistance to electron beam irradiation.

## II. EXPERIMENTAL

### A. Materials

LDPE, with a melting point of 112 °C, was supplied by the UBE Corporation, Japan. MH (Magnifin H10), with a median particle size of 0.80–1.10 μm, was obtained from the Albemarle Corporation. PBPP, with a polymerization degree of 2–3, was bought from Zibo Blue Chemical Company Limited, China.

### B. Composite preparation

LDPE-based composites were mixed with MH and PBPP in phr (phr = parts per hundred resin based on 100 parts of LDPE) by using a double roller mill SK-160B (Shanghai Rubber Machinery Works, China), with the roller rotor operating at 140 °C and 8 rpm for 10 min. After mixing, the composites were hot-pressed under 10 MPa into sheets with a thickness of 1 mm for 5 min at 160 °C. The composites are named as PE-*x*-*y*, where *x* stands for the phr value of the MH added and *y* is the phr value of the PBPP added. Details of the composites used in this work are listed in Table 1.

TABLE 1. Formulations

Composites	LDPE (phr)	MH (phr)	PBPP (phr)
PE-0-0	100	0	0
PE-20-0	100	20	0
PE-20-2.5	100	20	2.5
PE-20-5	100	20	5.0
PE-20-7.5	100	20	7.5
PE-20-10	100	20	10.0
PE-20-12.5	100	20	12.5
PE-50-0	100	50	0
PE-50-12.5	100	50	12.5

### C. Irradiation

Electron-beam irradiation of the samples was carried out in the air using a type of electron beam accelerator (KFG-1) at an acceleration voltage of 2.5 MeV and a current of 10 mA. The dose rate was 15 kGy for one pass. The total absorbed doses were in the range of 0–1000 kGy.

### D. Characterization

Fourier-transform infrared (FTIR) spectroscopy in the attenuated total reflectance (ATR) mode was employed to study

the chemical alterations occurring on the outer layer of the composite sheets. The FTIR-ATR measurements were performed on a Perkin Elmer Spectrum 100 FTIR spectrometer with a resolution of 4 cm<sup>-1</sup> and 32 scans per spectrum from 4000 cm<sup>-1</sup> to 500 cm<sup>-1</sup>.

Changes in the surface morphology were determined using a JEOL JSM-6500F scanning electron microscope (SEM). It was performed at an acceleration voltage of 10 kV. Prior to SEM examination, the samples were first cooled in liquid nitrogen to break and were then coated with a thin Au layer.

The density of the samples was measured on a Toyoceike automatic densitometer model DH-100 (Japan) according to ASTM D-1505.

Melt flow rate (MFR) tests were carried out according to ASTMD1238 in a SRZ-400E Melt Flow Tester (Changchun, China). Four automatically timed flow rate measurements were taken at a temperature of 190 °C by a load of 2.16 kg.

Tensile strength and elongation at the break of the composite samples were measured on an electronic tensile strength meter (5965, Instron, UK) equipped with a 500 N load cell, according to the ASTM D882-02 method, with a cross head speed of 250 mm/min and a gauge length of 20 mm at room temperature. For every composite, at least five samples were analyzed to obtain reproducible average values.

The limiting oxygen index (LOI) values were determined by using an HC-2 Oxygen Index instrument (Jiangning Analysis Instrument Factory, China) and the sample sheets were cut into 120 mm × 6 mm × 3 mm pieces according to ASTMD2863. The UL-94 horizontal vertical burning test was performed according to GB/T2408-1996 with a sample size of 130.0 mm × 13.0 mm × 1.6 mm on a CZF-3 type horizontal vertical burning test apparatus (Cangzhou Ke Shuo construction equipment Ltd., China).

Thermogravimetric analysis (TGA) was performed using a TG 209 F3 Tarsus Thermo-Microbalance (NETZSCH, Germany). The measurements were performed from room temperature to 700 °C at a heating rate of 10 °C/min under a nitrogen atmosphere.

## III. RESULTS AND DISCUSSION

### A. Chemical structure analysis

Figure 1 shows different spectra of the blend composites from 4000 cm<sup>-1</sup> to 500 cm<sup>-1</sup>. There was only a -CH<sub>2</sub>- functional group in the LDPE chains, so the ATR-FTIR spectrum of the MH-LDPE blend composite was observed at five main bands (Fig. 1c), the bands at 2918 cm<sup>-1</sup> and 2849 cm<sup>-1</sup> (CH<sub>2</sub> symmetrical and asymmetrical stretching), the band at 1465 cm<sup>-1</sup> (CH bending deformation), the band at 720 cm<sup>-1</sup> (CH rocking deformation), and the band at 3694 cm<sup>-1</sup>, which was -OH stretching vibration in the MH crystal. In the spectra of the PE-20-5 and PE-20-12.5 blend composites, the bands at 1590 cm<sup>-1</sup> and 1486 cm<sup>-1</sup> were attributed to the phenyl group framework's vibration, while the peaks at 767 cm<sup>-1</sup> and 685 cm<sup>-1</sup> were attributed to mono-substitution of the benzene ring. The bands at 1263 cm<sup>-1</sup> and 1176 cm<sup>-1</sup>

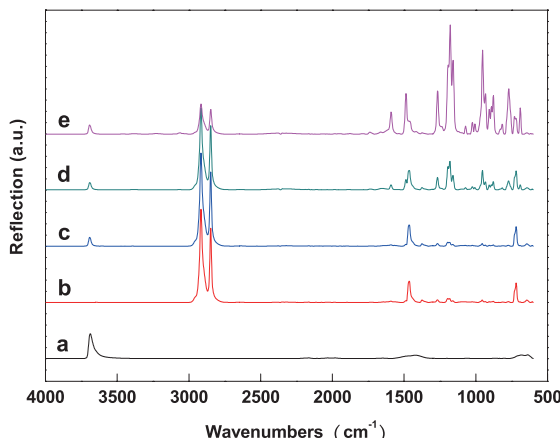


Fig. 1. (Color online) ATR- FTIR spectra of MH (a), LDPE (b), MH-LDPE (c) and PBPP-MH-LDPE (d, PE-20-5; e, PE-20-12.5) blend composites.

were attributed to P=N stretching (asymmetrical and symmetrical) and the band at 949 cm<sup>-1</sup> was attributed to the P—O—C stretching vibration in the side chain. The band at 774 cm<sup>-1</sup> was attributed to the P=N symmetrical stretching in the main chain of PBPP [18–21]. The presence of P=N and P—O—C peaks prove that PBPP existed in the LDPE blend composites. The intensities of the bands at 1263 cm<sup>-1</sup>, 1176 cm<sup>-1</sup> and 949 cm<sup>-1</sup> increased with increasing PBPP content in the LDPE blend composites because of the increasing functional group concentration of PBPP in the MH-LDPE blend composites.

### B. Morphology observation

Figure 2 illustrates the fractured surface morphologies of MH-LDPE blend composites filled with different loading levels of PBPP. Electron micrographs reveal that MH particles one micrometer or less in size were dispersed in the matrix. According to Fig. 2(a), there are many gaps existing between the MH particles and LDPE matrix due to incompatibility. The reason can be attributed to the MH particle being polar due to many hydroxyl groups existing on its surface. Conversely, the LDPE matrix is not polar. From Fig. 2(b) and Fig. 2(c), the gaps disappeared with PBPP adding. With the low loading of PBPP in Fig. 2(b), the PBPP matrix can not be observed clearly, and PBPP matrix is surrounded with MH particles. The PBPP matrix can be observed when loaded more PBPP, as seen in Fig. 2(c). It is suggested that PBPP be not compatible with the LDPE matrix. Fig. 2(d) is the cross section morphology of sample PE-20-12.5 after washing in ethanol. Some cavities were observed in Fig. 2(d) because PBPP can be dissolved in ethanol, while LDPE and MH can not, within a short period of time (for example 5 minutes). Meanwhile, there are many gaps that exist between MH particles and the LDPE matrix. It is proved that PBPP is covered on the MH particles. The SEM analysis revealed that PBPP exists between MH particles and the LDPE matrix, and possibly changes the interfacial interaction.

### C. MFR study

Melt flow rate (MFR) was used to characterize the processing properties. Figure 3 shows the variation of MFR values with the PBPP content at a constant MH loading of 20 phr. MFR increased with increasing PBPP loading in LDPE. The density was constant. As shown in Fig. 2(c) with the PBPP matrix covering the MH particles, the frictional resistance and the apparent viscosity in the flow cell decrease [22]. From Fig. 3, an increase in the PBPP content in the blend composites increase the melt flow rate, and when the content of PBPP is higher than 5.0 phr, the melt flow rate increases significantly due to some continuous PBPP phases in the LDPE matrix.

An increase in value of melt flow rate suggests that lower energy was consumed in blending extrusion and the subsequent molding process. Meanwhile, the production efficiency was improved accordingly. This result was significantly different from that of the addition of inorganic flame retardants only, which often resulted in severe deteriorated performance in materials processing. Of course, too much PBPP addition caused rapid deterioration of the mechanical properties of blend composites. After careful consideration, the content of PBPP with 5.0 phr is appropriate.

### D. Mechanical properties

The elongation at break of the blend composites was found to increase as PBPP content increased from 0 phr to 5.0 phr, as shown in Fig. 4(a). When PBPP was added in MH-LDPE blends, the PBPP matrix covered the MH particles, as seen previously in the SEM figures. Thus PBPP reduced the frictional force during the stretching process and the elongation at break for the blend increased. However, further increase of PBPP content in the blends caused a decrease in elongation at break. Because the PBPP phase deteriorated, the LDPE was a continuous phase. The trend of elongation at break for the blends is in agreement with the previous report [23]. The tensile strength in Fig. 4(b) showed a downward trend with the increasing PBPP content, as that PBPP matrix covered the MH particles, the friction force between the MH particles and the LDPE matrix was reduced. At 200 kGy absorbed dose, the elongation of blend composites is lower than that at 0 kGy, but the tensile strength is higher than that at 0 kGy, due to the crosslink of LDPE.

In this study, we found that the elongation at break varied greatly from the variation of PBPP content and reached the maximum at around 5.0 phr at 0 kGy and 200 kGy. So 5.0 phr PBPP is appropriate in LDPE blend composites containing 20 phr MH.

### E. Flammability

The flammability of blend composites was investigated by LOI and UL-94 burning. The results are listed in Table 2. The LOI of blend composites increases with the increasing

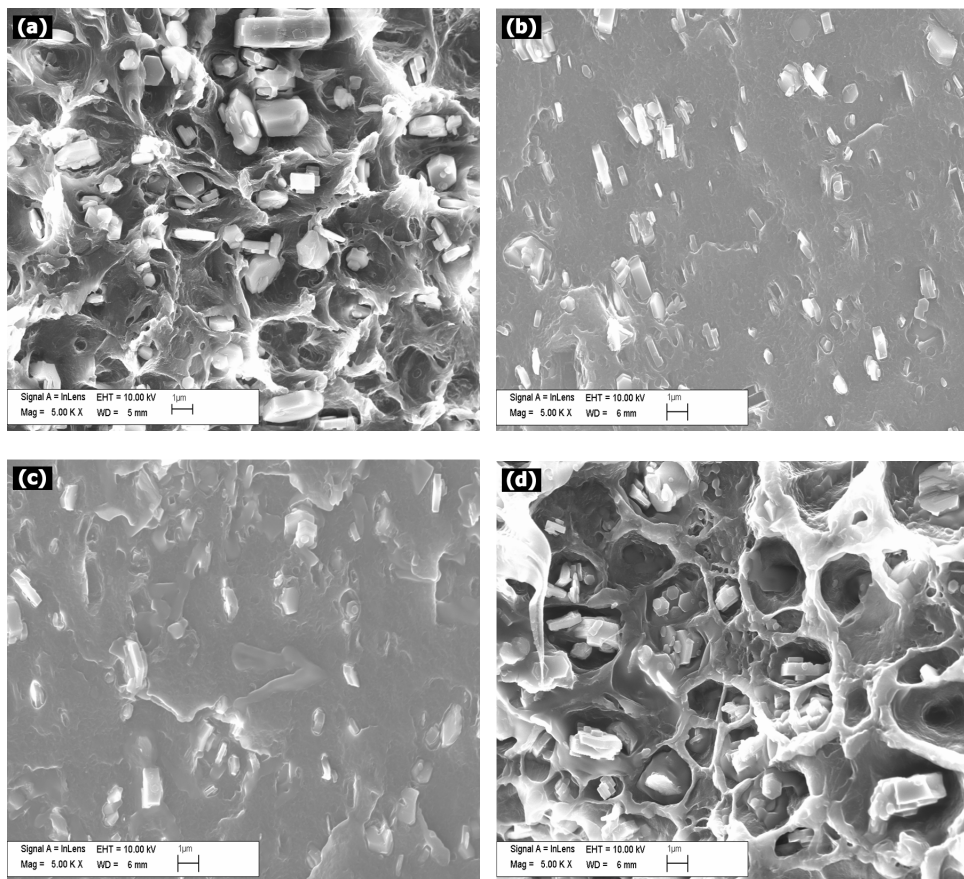


Fig. 2. SEM micrographs of MH-LDPE (a), and PBPP-MH-LDPE ((b) PE-20-2.5, (c) PE-20-12.5, (d) PE-20-12.5 after washing in ethanol) composites (Mag = 5.00 K).

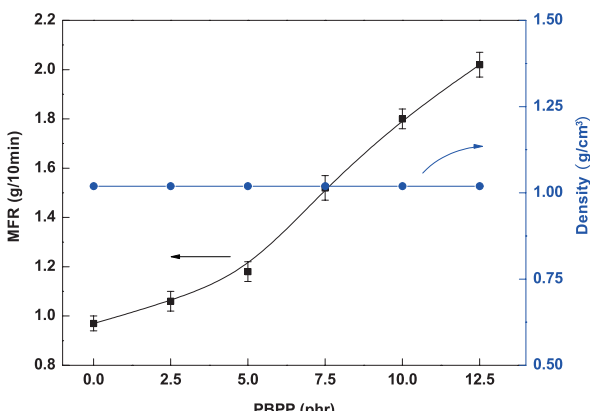


Fig. 3. (Color online) MFR and Density values of blend composites with different PBPP content at 20 phr MH.

of the MH loading level. The LOI of PBPP-containing composites is higher than that of non-PBPP. The UL-94 burning data shows that only PE-50-12.5 reached V2. There is no molten drop during combustion. This indicates that the PBPP have anti dripping abilities. The decomposition and dehydration reactions of MH happened during the combustion pro-

TABLE 2. The flammability of LDPE and PBPP-MH-LDPE blend composites

Sample	LOI (%)		UL-94		Molten Drops	
	0 kGy	200 kGy	0 kGy	200 kGy	0 kGy	200 kGy
PE-0-0	17.5	18	-	-	Yes	Yes
PE-20-0	19	19.6	-	-	Yes	Yes
PE-20-5	20	20.7	-	-	No	No
PE-50-0	22.2	23	-	-	Yes	Yes
PE-50-12.5	24.3	25	V2	V2	No	No

Yes: With molten drops; No: Without molten drops

cess. The MH particles reduced the surface temperature of the burning material by absorbing heat from the surface of the polymer material. The amount of steam produced from dehydration of MH diluted the concentration of combustible gas and oxygen. After decomposition, the residues-dense ( $\text{MgO}$ ) was deposited on the polymer matrix surface. This not only played an important role in heat insulation and as an oxygen barrier, but also suppressed smoke. Besides, MH could improve polymer surface charring [24–29].

Since PBPP showed many advantages: halogen-free, low toxicity, low smoke, good stability on UV-rays, and good flame retardant efficiency, it was selected as a flame retardant.

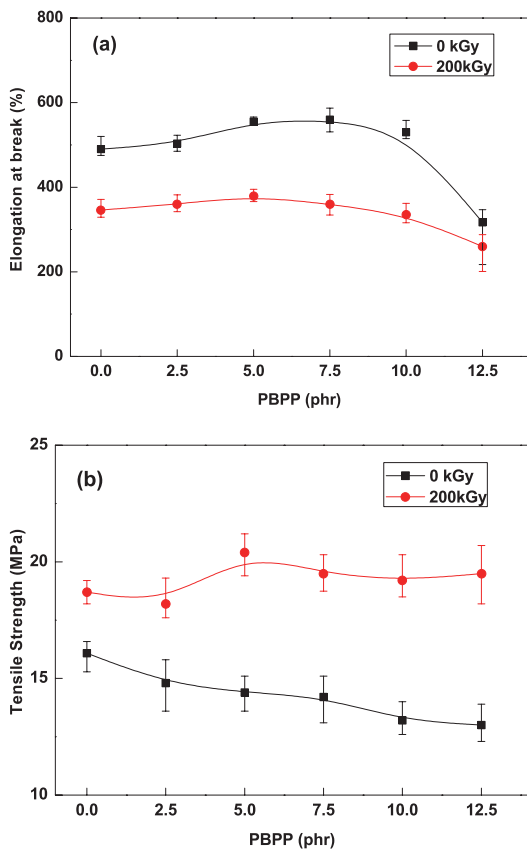


Fig. 4. (Color online) Elongation at break (a) and tensile strength (b) of blend composites with different PBPP content at 0 kGy and 200 kGy.

As soon as it is subjected to heat or combustion, phosphorus-containing compounds can turn to oxygen acids of phosphorus by thermal decomposition. The generated metaphosphoric acid is a stable polymeric phosphatic acid, which prevents the surface of the composite material being exposed to oxygen and combustibles. In addition, the heated phosphorus compound can emit  $\text{PO}_\cdot$  radicals, which are able to capture  $\text{OH}^-$ ,  $\text{H}\cdot$  etc., in the combustion chain reaction [30–33]. Nitrogen in PBPP produces non-combustible gases by decomposition, such as  $\text{NH}_3$ ,  $\text{N}_2$ ,  $\text{NO}$ ,  $\text{NO}_2$ , etc. These gases dilute the concentration of oxygen and combustibles in air and absorb heat during the decomposition of retardants. This process could reduce the surface temperature of the substrate. Meanwhile, the nitrogen oxides, through decomposition, could capture free radicals and inhibit combustion chain reactions in polymer composites. Therefore, the PBPP flame retardant can be cooled by gas dilution, the formation of insulation, termination of radical chain reactions, and other ways to achieve flame retardant properties [34–36].

#### F. Property changes after irradiation

The polymer chain of PBPP was constituted by a conjugated structure of repeating  $-\text{P}=\text{N}-$ . There are lots of benzene

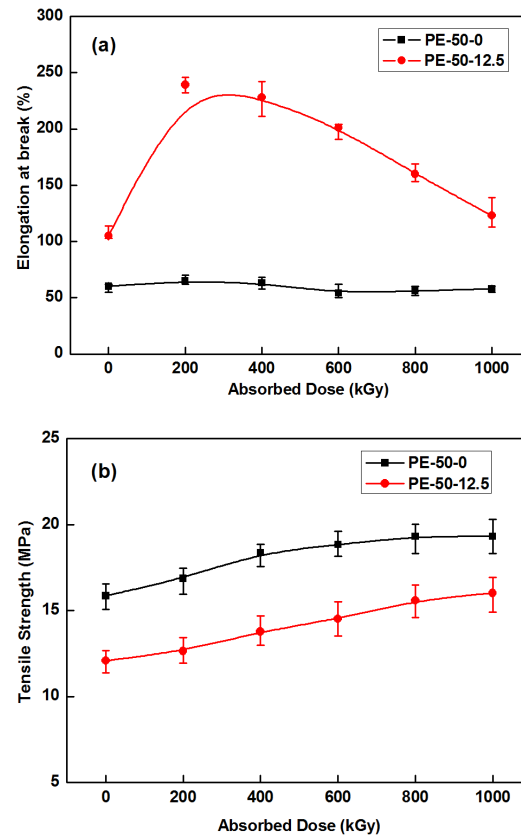


Fig. 5. (Color online) Elongation at break (a) and tensile strength (b) of PE-50-0 and PE-50-12.5 blend composites at different absorbed dose.

rings in the side chains. A benzene ring is a conjugated structure with a rich electron cloud. With large electron cloud systems, PBPP could resist and scatter electron beams. The anti-irradiation properties of the materials were investigated by elongation at break. Figure 5(a) shows the elongation results of PE-50-0 and PE-50-12.5 samples at different absorbed doses. It shows that the elongation of PBPP-containing blend composites is evidently higher than that of non-PBPP. The value of elongation of the PE-50-12.5 blended composite reached the maximum, 200 kGy. Dominated by cross-linking in the LDPE matrix at 200 kGy absorbed doses, thereafter, the degradation increases with the absorbed doses. The tensile strength in Fig. 5(b) increased with the absorbed doses. However, the tensile strength of the PBPP-containing blend composites was lower than that of non-PBPP. This can be explained by the data in Fig. 4(b).

To illustrate the role of PBPP in irradiation, thermal gravimetric analysis (TGA) was employed. In Fig. 6(b), a two-step degradation (385–420 °C and 430–505 °C, respectively) was found. The first step degradation was attributed to PBPP and the second degradation step was attributed to LDPE. A significant change in the first step degradation was found that the content of PBPP was reduced by increasing doses from 0 kGy to 1000 kGy. Furthermore, the degradation step changed from 385–420 °C to 365–400 °C in the curve of

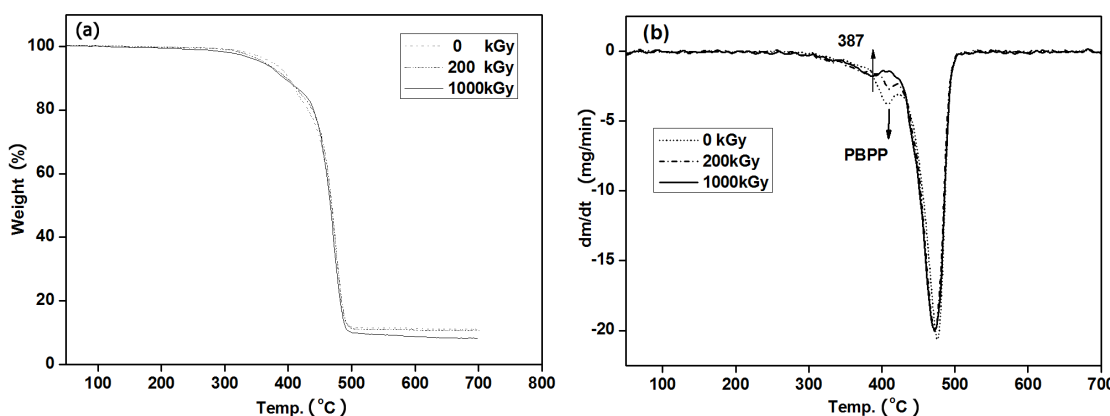


Fig. 6. TGA (a) and DTG (b) profiles of PBPP-MH-LDPE blend composites at different absorbed doses.

1000 kGy. This was due to the lower molecular weight of PBPP through irradiation. From the results of DTG, it can be concluded that PBPP can protect the LDPE polymer matrix by consuming itself.

#### IV. CONCLUSION

The effects of PBPP in MH-LDPE blend composites on the flame retardance and electron beam irradiation were examined. The melt flow rate (MFR) and scanning electron microscope (SEM) were employed to characterize the processing properties and morphology of the blend composites. The mechanical properties test and TGA were used to analyze the

irradiated blend composites. The main conclusions of this work are:

- (1) As the PBPP content in the blend increases, the melt flow rate increases. It indicated that the existence of PBPP favors the interfacial interaction between LDPE and MH.
- (2) According to the elongation at break of blend composites at different ratios, the appropriate content of PBPP was around 5.0 phr at 20 phr MH.
- (3) The values of the limiting oxygen index (LOI) increased with the PBPP content.
- (4) PBPP has a positive effect on the resistance of electron beam irradiation by consuming itself.

---

[1] Lujan-Acosta R, Sánchez-Valdes S, Ramírez-Vargas E, et al. Effect of amino alcohol functionalized polyethylene as compatibilizer for LDPE/EVA/clay/flame-retardant nanocomposites. *Mater Chem Phys*, 2014, **146**: 437–445. DOI: [10.1016/j.matchemphys.2014.03.050](https://doi.org/10.1016/j.matchemphys.2014.03.050)

[2] Haurie L, Fernández A I, Velasco J I, et al. Thermal stability and flame retardancy of LDPE/EVA blends filled with synthetic hydromagnesite/aluminium hydroxide/montmorillonite and magnesium hydroxide/aluminium hydroxide/montmorillonite mixtures. *Polym Degrad Stabil*, 2007, **92**: 1082–1087. DOI: [10.1016/j.polymdegradstab.2007.02.014](https://doi.org/10.1016/j.polymdegradstab.2007.02.014)

[3] Lu S Y and Hamerton I. Recent developments in the chemistry of halogen-free flame retardant polymers. *Prog Polym Sci*, 2002, **27**: 1661–1712. DOI: [10.1016/s0079-6700\(02\)00018-7](https://doi.org/10.1016/s0079-6700(02)00018-7)

[4] Jurs J L and Tour J M. Novel flame retardant polyarylethers: synthesis and testing. *Polymer*, 2003, **44**: 3709–3714. DOI: [10.1016/s0032-3861\(03\)00277-5](https://doi.org/10.1016/s0032-3861(03)00277-5)

[5] Riva A, Camino G, Fomperie L, et al. Fire retardant mechanism in intumescent ethylene vinyl acetate compositions. *Polym Degrad Stabil*, 2003, **82**: 341–346. DOI: [10.1016/s0141-3910\(03\)00191-5](https://doi.org/10.1016/s0141-3910(03)00191-5)

[6] Hu X P, Li W Y and Wang Y Z. Synthesis and characterization of a novel nitrogen-containing flame retardant. *J Appl Polym Sci*, 2004, **94**: 1556–1561. DOI: [10.1002/app.20792](https://doi.org/10.1002/app.20792)

[7] Fitzsimmons B W and Shaw R A. Phosphorus-nitrogen compounds. Part VII. Alkoxy- and aryloxy-cyclophosphazenes. *J Chem Soc*, 1964, 1735–1741. DOI: [10.1039/JR9640001735](https://doi.org/10.1039/JR9640001735)

[8] Liu Y L, Liu Y L, Jeng R J, et al. Triphenylphosphine oxide-based bismaleimide and poly(bismaleimide): synthesis, characterization, and properties. *J Polym Sci Pol Chem*, 2001, **39**: 1716–1725. DOI: [10.1002/pola.1149](https://doi.org/10.1002/pola.1149)

[9] Chiang C L and Ma C C M. Synthesis, characterization and thermal properties of novel epoxy containing silicon and phosphorus nanocomposites by sol-gel method. *Eur Polym J*, 2002, **38**: 2219–2224. DOI: [10.1016/s0014-3057\(02\)00123-4](https://doi.org/10.1016/s0014-3057(02)00123-4)

[10] Lin C H and Wang C S. Novel phosphorus-containing epoxy resins Part I. Synthesis and properties. *Polymer*, 2001, **42**: 1869–1878. DOI: [10.1016/S0032-3861\(00\)00447-X](https://doi.org/10.1016/S0032-3861(00)00447-X)

[11] Sasuga T and Hagiwara M. Molecular motion of non-crystalline poly(aryl ether-ether-ketone) PEEK and influence of electron-beam irradiation. *Polymer*, 1985, **26**: 501–505. DOI: [10.1016/0032-3861\(85\)90148-x](https://doi.org/10.1016/0032-3861(85)90148-x)

[12] Sasuga T, Hayakawa N, Yoshida K, et al. Degradation in tensile properties of aromatic polymers by electron-beam irradiation. *Polymer*, 1985, **26**: 1039–1045. DOI: [10.1016/0032-3861\(85\)90226-5](https://doi.org/10.1016/0032-3861(85)90226-5)

[13] Sasuga T and Hagiwara M. Mechanical relaxation of crystalline poly(aryl ether-ether-ketone) PEEK and influence of electron-beam irradiation. *Polymer*, 1986, **27**: 821–826. DOI: [10.1016/0032-3861\(86\)90288-0](https://doi.org/10.1016/0032-3861(86)90288-0)

[14] Heiland K, Hill D J T, Hopewell J L, et al. Measurement of radical yields to assess radiation resistance in engineering thermoplastics. In: Clough R L, Billingham N C, Gillen K T, editors. *Polymer Durability*. Washington (USA): American Chemical Society, 1996, 637–649.

[15] Zhang X H, Chen S, Min Y Q, et al. Synthesis of novel bisphenol containing phthalazinone and azomethine moieties and thermal properties of cured diamine/bisphenol/DGEBA polymers. *Polymer*, 2006, **47**: 1785–1795. DOI: [10.1016/j.polymer.2006.01.075](https://doi.org/10.1016/j.polymer.2006.01.075)

[16] El-Sayed S M and Madani M. Effect of dosage on the conduction of electron beam cross-linked thermoplastic elastomeric films from blend of LDPE and EVA copolymer. *Mater Manuf Process*, 2008, **23**: 163–168. DOI: [10.1080/10426910701774668](https://doi.org/10.1080/10426910701774668)

[17] Sabet M, Hassan A and Ratnam C T. Mechanical, electrical, and thermal properties of irradiated low-density polyethylene by electron beam. *Polym Bull*, 2012, **68**: 2323–2339. DOI: [10.1007/s00289-012-0741-y](https://doi.org/10.1007/s00289-012-0741-y)

[18] Ye L and Wu Q H. Effects of an intercalating agent on the morphology and thermal and Flame-Retardant properties of low-density polyethylene/layered double hydroxide nanocomposites prepared by melt intercalation. *J Appl Polym Sci*, 2012, **123**: 316–323. DOI: [10.1002/app.33770](https://doi.org/10.1002/app.33770)

[19] Rajandas H, Parimannan S, Sathasivam K, et al. A novel FTIR-ATR spectroscopy based technique for the estimation of low-density polyethylene biodegradation. *Polymer Testing*, 2012, **31**: 1094–1099. DOI: [10.1016/j.polymertesting.2012.07.015](https://doi.org/10.1016/j.polymertesting.2012.07.015)

[20] Dez I and De Jaeger R. Synthesis and radical polymerization of methacrylate monomers containing cyclotriphosphazene. Thin-layer grafts of their polymers on a poly(vinyl alcohol) surface. *Macromolecules*, 1997, **30**: 8262–8269. DOI: [10.1021/ma9707042](https://doi.org/10.1021/ma9707042)

[21] Chen-Yang Y W, Lee H F and Yuan C Y. A flame-retardant phosphate and cyclotriphosphazene-containing epoxy resin: synthesis and properties. *J Polym Sci Pol Chem*, 2000, **38**: 972–981. DOI: [10.1002/\(SICI\)1099-0518\(20000315\)38:6<972::AID-POLA6>3.0.CO;2-N](https://doi.org/10.1002/(SICI)1099-0518(20000315)38:6<972::AID-POLA6>3.0.CO;2-N)

[22] Duan Y F and Fu Z X. Influence of poly(*n*-octadecyl acrylate) on mechanical properties, melting behavior, and morphology of polypropylene/aluminum trihydroxide composites. *Fire Mater*, 2012, **36**: 614–622. DOI: [10.1002/FAM.1121](https://doi.org/10.1002/FAM.1121)

[23] Lai S M, Yeh F C, Wang Y, et al. Comparative study of maleated polyolefins as compatibilizers for polyethylene/wood flour composites. *J Appl Polym Sci*, 2003, **87**: 487–496. DOI: [10.1002/app.11419](https://doi.org/10.1002/app.11419)

[24] Miyata S, Imahashi T and Anabuki H. Fire-retarding polypropylene with magnesium-hydroxide. *J Appl Polym Sci*, 1980, **25**: 415–425. DOI: [10.1002/app.1980.070250308](https://doi.org/10.1002/app.1980.070250308)

[25] Titelman G I, Gonen Y, Keidar Y, et al. Discolouration of polypropylene-based compounds containing magnesium hydroxide. *Polym Degrad Stabil*, 2002, **77**: 345–352. DOI: [10.1016/s0141-3910\(02\)00064-2](https://doi.org/10.1016/s0141-3910(02)00064-2)

[26] Rothon R N and Hornsby P R. Flame retardant effects of magnesium hydroxide. *Polym Degrad Stabil*, 1996, **54**: 383–385. DOI: [10.1016/s0141-3910\(96\)00067-5](https://doi.org/10.1016/s0141-3910(96)00067-5)

[27] Greda O, Horvathova E, Besinova O, et al. Flame retardant treated plywood. *Polym Degrad Stabil*, 1999, **64**: 529–533. DOI: [10.1016/s0141-3910\(98\)00152-9](https://doi.org/10.1016/s0141-3910(98)00152-9)

[28] Hornsby P R and Watson C L. Mechanism of smoke suppression and fire retardancy in polymers containing magnesium-hydroxide filler. *Plast Rub Process Appl*, 1989, **11**: 45–51.

[29] Ahamad A, Patil C B, Mahulikar P P, et al. Studies on the flame retardant, mechanical and thermal properties of ternary magnesium hydroxide/clay/EVA nanocomposites. *J Elastom Plast*, 2012, **44**: 251–261. DOI: [10.1177/0095244311424553](https://doi.org/10.1177/0095244311424553)

[30] Weil E D, Levchik S V, Ravey M, et al. A survey of recent progress in phosphorus-based flame retardants and some mode of action studies. *Phosphorus Sulfur*, 1999, **144**: 17–20. DOI: [10.1080/10426509908546171](https://doi.org/10.1080/10426509908546171)

[31] Green J. A review of phosphorus-containing flame retardants. *J Fire Sci*, 1992, **10**: 470–487. DOI: [10.1177/073490419201000602](https://doi.org/10.1177/073490419201000602)

[32] Aaronson A M and Bright D A. Oligomeric phosphate esters as flame retardants. *Phosphorus Sulfur*, 1996, **109**: 83–86. DOI: [10.1080/10426509608545096](https://doi.org/10.1080/10426509608545096)

[33] Troitzsch J. Flame-retardant polymers current status and future-trends. *Makromol Chem-M Symp*, 1993, **74**: 125–135. DOI: [10.1002/masy.19930740115](https://doi.org/10.1002/masy.19930740115)

[34] Horacek H and Grabner W. Nitrogen based flame retardant for nitrogen-containing polymers. *Makromol Chem-M Symp*, 1993, **74**: 271–276. DOI: [10.1002/masy.19930740131](https://doi.org/10.1002/masy.19930740131)

[35] Sivrev C and Žabski L. Flame retarded rigid polyurethane foams by chemical modification with phosphorus-containing and nitrogen-containing polyols. *Eur Polym J*, 1994, **30**: 509–514. DOI: [10.1016/0014-3057\(94\)90053-1](https://doi.org/10.1016/0014-3057(94)90053-1)

[36] Von Gentzkow W, Huber J, Kapitza H, et al. Halogen-free flame-retardant plastics for electronic applications. *J Vinyl Addit Techn*, 1997, **3**: 175–178. DOI: [10.1002/vnl.10185](https://doi.org/10.1002/vnl.10185)